Reciprocal Activation of Breast Cancer Metastases and the Lung Epithelium During Metastatic Outgrowth

Jessica L. Christenson, Nicole S. Spoelstra, Kathleen I. O'Neill, Michelle M. Williams, Jennifer K. Richer
University of Colorado, School of Medicine, Department of Pathology

University of Colorado Anschutz Medical Campus

Introduction

- No metastasis-specific therapeutic strategies are currently available.
- The lung is one of the most common sites of breast cancer (BC) metastasis.
- Triple-negative breast cancers (TNBC) preferentially metastasize to the lung.
- The overall prognosis for BC patients diagnosed with metastatic disease is 2-3 years; those with lung metastases have a prognosis of approximately 1 year.
- BC cells metastasize to the peripheral tissue of the lung, commonly to the lung parenchyma where alveoli are a central component.
- Type II alveolar epithelial (AT2) cells are the most numerous cells within the alveolus and are likely to interact extensively with metastatic cells in the lung.

- **How established micrometastases remodel the lung microenvironment and how this contributes to metastatic outgrowth is not well understood.**
- We identified a connection between metastatic outgrowth and aberrant lung wound healing that has revealed multiple tangible targets for intervention.

Hypothesis

We hypothesize that BC metastases activate surrounding lung epithelial cells which, in turn, support the survival and outgrowth of metastases within the lung.

Overall Goal

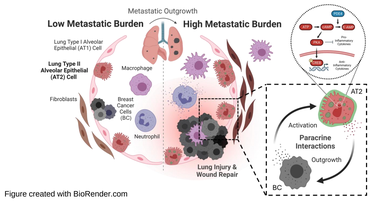

Figure created with BioRender.com

The overall goal of these studies is to identify factors secreted by lung epithelial cells that could be targeted to reduce metastatic outgrowth and thereby improve patient survival and quality of life.

Methods

Mouse Models of BC Metastasis

- MMTV-PyMT (mouse mammary tumor virus-polyoma middle T antigen) transgenic mice: Develop spontaneous mammary tumors that metastasize to the lung.
- Late-stage metastasis model: Met-1 mouse mammary carcinoma cells, originally isolated from a MMTV-PyMT primary tumor, were injected into the tail veins of immunocompetent, syngeneic female FVB/NJ mice.

Metastasis-Associated Wound Repair Analysis

Custom multispectral fluorescent imaging panels were used to quantify metastasis-associated wound repair and type II alveolar epithelial (AT2) cell activation in the lung directly adjacent to metastases.

Single Cell RNA-sequencing (scRNAseq)

Lungs from mice with a low or high metastatic burden, using the late-stage metastasis model, were dissociated and RNA expression was measured for individual cells by scRNAseq. Approximately 3,000 cells per sample were sequenced with a read-depth of ~125,000 reads/cell via the 10X Genomics platform and Illumina NovSeq 6000 platforms (University of Colorado's Genomics and Sequencing Core). Read mapping and expression quantification were performed using a combination of the 10X Cellranger pipeline and custom analytic scripts.

Co-Culture Model

Human A549 lung carcinoma cells were cultured for >8 passages to shift them into a more epithelial AT2 cell phenotype. Human iPSC (induced pluripotent stem cells) were differentiated to lung AT2 cells. Lysotracker was used to stain AT2-specific lamellar bodies to verify differentiation. No contact co-culture experiments were performed for 5-7 days. TNBC cell numbers were measured using the crystal violet cell viability assay and iAT2 gene expression changes were determined by bulk RNAseq.

Indicators of wound repair and AT2 cell activation develop in the lung during metastatic outgrowth

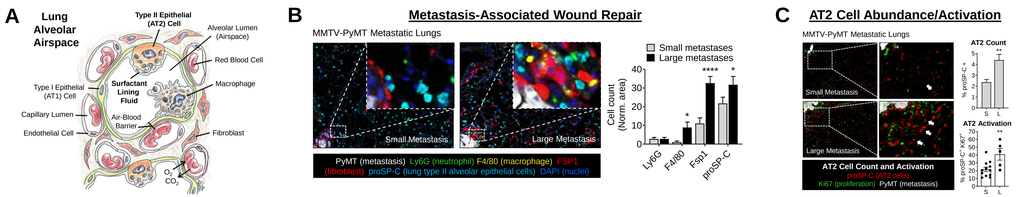

Figure 1. (A) Illustration of the cellular components and key features of lung alveoli; adapted from Harkema *et al.* 2019. **(B)** MMTV-PyMT lung metastases were separated by size (S, small: diameter <150μm and L, large >300μm) and stained by multispectral immunofluorescent (IF) imaging. Adjacent cell counts (within 300μm) were normalized to area, n=8 metastases from 6 mice. **(C)** MMTV-PyMT metastatic lungs co-stained for proSP-C, Ki67 and PyMT using multispectral IF imaging. The percentage of proSP-C+ AT2 cells (as a % of total cells) and proSP-C+Ki67+ activated AT2 cells (arrows, as a % of total AT2 cells) were quantified; n=6 mice. Mean ± SEM; * p<0.05, ** p<0.01, **** p<0.0001.

Paracrine interactions between lung AT2 cells and BC cells

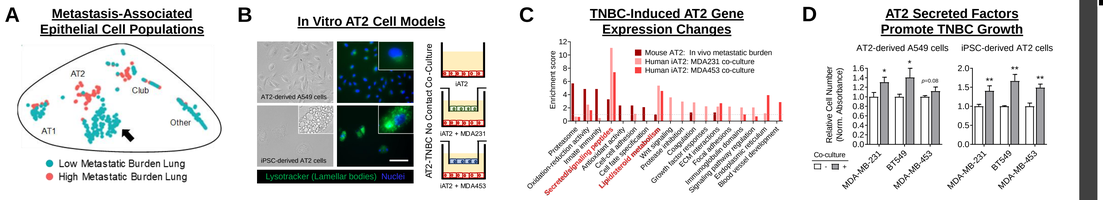

Figure 2. (A) scRNAseq comparing lungs with a low vs high metastatic burden (n=1 mouse/group) using MMTV-PyMT-derived Met-1 mouse mammary carcinoma cells injected intravenously (IV). Epithelial cells clustered by gene expression (arrow indicating AT2 cells). **(B)** Human AT2 cell models for studying the reciprocal effects of secreted factors on human AT2 and TNBC cells. Lysotracker was used to verify AT2 cell status by staining AT2-specific lysosome-like lamellar bodies. Scale bar = 50μm; iPSC, induced pluripotent stem cells. **(C)** Bulk RNAseq was performed on AT2 cells no-contact co-cultured for 3 days with MDA-MB-231 (MDA231) and MDA-MB-453 (MDA453) TNBC cells. The most significantly altered functional pathways for mouse AT2 scRNAseq and no-contact co-cultured human AT2 cell bulk RNAseq. Upregulation of secreted peptide and lipid metabolism pathways was observed in all three datasets. **(D)** TNBC cell growth following no-contact co-cultured with human AT2 cells for 5-7 days, normalized to cells cultured alone; mean ± SD, * p<0.05, ** p<0.01.

Activation by BC cells alters AT2-derived pulmonary surfactant composition and surfactant supplementation inhibits BC cell viability

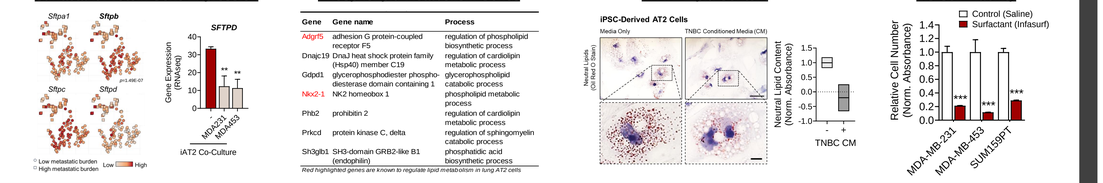

Gene	Gene name	Process
Adgrf5	adhesion G protein-coupled receptor F5	regulation of phospholipid biosynthetic process
Dnajc19	DnaJ heat shock protein family (Hsp40) member C19	regulation of cardiolipin metabolic process
Gdpd1	glycerophosphodiester phospho-diesterase domain containing 1	glycerophospholipid catabolic process
Nkx2-1	NK2 homeobox 1	phospholipid metabolic process
Phb2	prohibitin 2	regulation of cardiolipin metabolic process
Prkcd	protein kinase C, delta	regulation of sphingomyelin catabolic process
Sh3glb1	SH3-domain GRB2-like B1 (endophilin)	phosphatidic acid biosynthetic process

Red highlighted genes are known to regulate lipid metabolism in lung AT2 cells

Figure 3. (A) Surfactant protein (Sftp) gene expression differences in AT2 cells from the lung scRNAseq dataset and surfactant protein D (*SFTPD*) gene expression in AT2 cells no-contact co-cultured with TNBC cells from the bulk RNAseq dataset. **(B)** Mouse lung metastasis scRNAseq data indicates that several phospholipid metabolism genes are altered in AT2 cells during metastatic outgrowth, including some directly related to surfactant metabolism (in red). **(C)** AT2 cells were cultured in media alone or a 50% dilution of conditioned media (CM) from MDA-MB-231 cells for 3 days. Neutral lipid content was measured by Oil Red O stain; scale bar = 50μm, inset scale bar = 10μm. Lipid stain was quantified as relative absorbance; median. **(D)** TNBC cell viability in a 50% dilution of the pulmonary surfactant for 5 days; normalized to control cells for each cell line. Mean ± SD, ** p<0.01, *** p<0.001.

BC-induced lung inflammation and *PDE4* expression

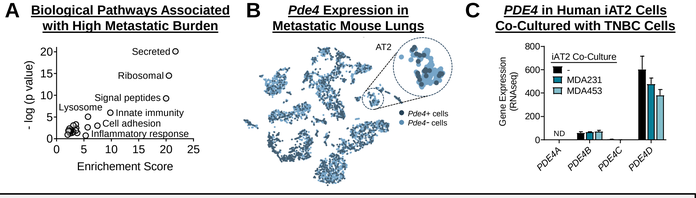

Figure 4. (A) scRNAseq gene expression data from all lung cell types combined by condition (low versus high metastatic burden) indicating the biological pathways most highly associated with metastatic outgrowth. **(B)** scRNAseq data colored by *Pde4* (phosphodiesterase 4) expression, all isoform levels combined, depicting the wide distribution of *Pde4* in mouse lung cell types, including AT2 cells. **(C)** *PDE4* isoform gene expression in AT2 cells no-contact co-cultured for 3 days with TNBC cells from the bulk RNAseq dataset. Mean ± SEM; ND, not detectable.

Targeting metastatic BC growth with the anti-inflammatory PDE4 inhibitor Roflumilast

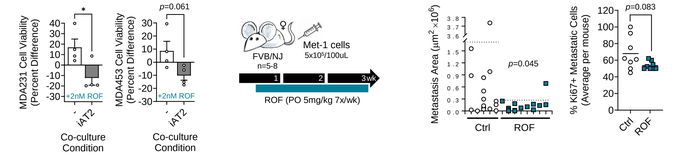

Figure 5. (A) TNBC cells were no-contact co-cultured with human iAT2 cells and treated with a biologically relevant dose of 2nM roflumilast (ROF) for 7 days. Control cells were cultured alone and/or treated with vehicle alone. TNBC viability was measured by absorbance and the effect of ROF on cell viability, as measured by the percent difference between vehicle and ROF treated cells, was calculated. Mean ± SEM, * p<0.05. **(B)** Met-1 mouse mammary carcinoma cell model of a late-stage metastasis with anti-inflammatory intervention, n=5-8 mice per group. Following metastatic colonization, mice were treated daily with oral ROF or vehicle control (Ctrl). **(C)** The number and size of metastases were measured per mouse. Each tick on the x-axis represents one mouse and each dot represents an individual metastasis. The dotted lines represent the mean per group. Proliferation of lung metastases was measured by quantifying the percentage of Ki67-positive stained cells, mean average per mouse.

Conclusions and Future Directions

- Aberrant wound repair develops during metastatic outgrowth.
- Lung AT2 cells adjacent to growing metastases become activated and undergo significant pro-tumor alterations to their secretome.
- AT2 secreted factors promote tumor cell growth.
- AT2 pulmonary surfactant protein and lipid levels are altered by BC-derived secreted factors and surfactant supplementation inhibits TNBC cell viability.
- Metastasis-associated wound repair and AT2-induced tumor cell proliferation can be blocked by the anti-inflammatory PDE4 inhibitor roflumilast.
- **Summary: Our studies demonstrate that targeting lung epithelial cells in the metastatic microenvironment may be an effective way to treat BC lung metastases.**
- Future studies will elucidate how activated resident lung cells support metastatic progression and may lead to the development and/or repurposing of clinically relevant therapeutic strategies to prevent destructive metastatic outgrowth within the lung.